Photocatalytic degradation of fast green dye using green synthesized nickel oxide nanoparticles

Paliwal Gaurav*, Ameta Neeraj and Tak Paras
Department of Chemistry, Pacific Academy of Higher Education and Research University, Udaipur -313003 (Raj.), INDIA
*grvplwl@gmail.com

Abstract
This study explores the photocatalytic degradation of Fast Green FCF dye using nickel oxide (NiO) nanoparticles synthesized through a green synthesis approach. The efficiency of the degradation process was found to be influenced by several parameters including pH, the amount of NiO catalyst, dye concentration and light intensity. Radical scavenging experiments revealed that hydroxyl radicals are primarily responsible for the dye's degradation.

The reaction kinetics was monitored using spectrophotometers and followed a pseudo-first-order model. The photocatalytic process was sensitive to variations in operational conditions such as catalyst dosage, dye concentration, pH level and light exposure. Experimental evidence supports a photochemical mechanism for the breakdown of Fast Green FCF.

Keywords: Fast Green dye, Nickel Nitrate, XRD, FESEM, EDS, FT-IR Photocatalytic Degradation.

Introduction

The presence of synthetic dyes in wastewater is rapidly increasing due to the extensive use of clothing and consumer products, making it a major global environmental concern.[21,22] Photocatalytic technology has attracted growing interest for its potential applications in environmental and energy-related fields, providing a simple and cost-effective method for pollution treatment.[13,16] Photocatalysis has been extensively investigated for over a century.[1,9] A photocatalyst is a substance that enhances the rate of a chemical reaction upon activation by UV-visible light, producing electron-hole pairs that drive redox processes.[5,22]

Current research continues to expand into novel catalytic reactions. Spinel-type materials are of particular interest due to their notable catalytic and magnetic characteristics. Among these, spinel cobaltites have shown remarkable catalytic performance, as highlighted by Hyeon.[9] A key method for synthesizing cobaltites involves thermal treatment of co-precipitated precursors.[11,14]

Various synthesis techniques for spinels have been explored including complexometric (sol-gel) methods using glycolates, EDTA and co-precipitation of hydroxides and oxalates, as well as methods involving fumarate and citrate intermediates.[12,18] Additional approaches include organometallic synthesis within polymer matrices, mechanochemical methods using binary oxides and synthesis inside silica ampoules.[2,7] Significant research attention has also been directed toward the synthesis of nickel oxide systems, focusing on variables such as precursor selection, synthesis routes, process control and calcination temperatures.[3,4]

Among the binary transition metal spinel oxides with the general formula MCo_2O_4, MFe_2O_4 and MCr_2O_4, where M represents a divalent d-block metal ion, cobaltites of nickel, copper and zinc are particularly noteworthy due to their versatile applications in fields such as electrode materials, magnetics, thermistors and catalysis.[6,17,23] Nigrosin dye, widely used in applications like lacquers, coatings, marker inks, textiles and biological studies, also garners interest in this context.

Fast Green Dye:

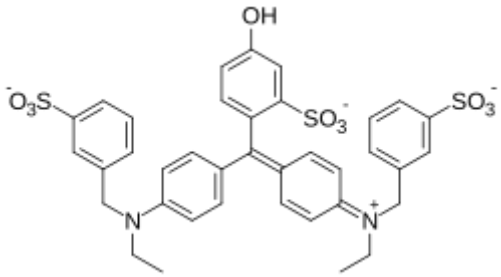

Fig. 1: Chemical Structure of Fast Green Dye

Fast Green (also known as Solvent Black 5) is a synthetic black dye composed of a mixture of related compounds, typically produced by heating nitrobenzene, aniline and hydrochloric acid in the presence of copper or iron catalysts. It is primarily used industrially as a colouring agent in lacquers, varnishes and marker pen inks. When sulfonated, Fast Green becomes a water-soluble anionic dye. In addition to its main industrial applications; small quantities of Fast Green are used in microbiology for negative staining of bacteria and for visualizing the encapsulated fungus *Cryptococcus neoformans*. In these staining techniques, the dye provides a dark background, allowing the transparent outlines of cells and fungi to be clearly observed. Fast Green WS is also employed in cell viability assays, as it is excluded by living cells but penetrates and stains dead ones.

Material and Methods

Materials: All the chemical reagents used in the synthesis were of analytical grade. Nickel nitrate.$6H_2O$ was used without further purification.

Table 1
Chemical Properties of Fast Green

IUPAC Name	Sodium [4-[[(4-(dimethylamino)phenyl)-(4-hydroxy-2-sulfonatophenyl) methylidene]amino]phenyl]ethenesulfonate
Chemical Formula	$C_{37}H_{34}N_2Na_2O_{10}S_3$
Molar Mass	808.85 g/mol
Melting Point	290 °C
Solubility	Soluble in water, slightly soluble in ethanol
λ_{max}	625 nm

Preparation of Rose Leaf Extract: Rose leaves were collected from the Haldighati region in Rajasthan and thoroughly washed with running tap water to remove dirt and surface contaminants, followed by rinsing with distilled water. The leaves were then shade-dried at room temperature to eliminate residual moisture. For the preparation of the aqueous extract, 100 g of the dried leaves were cut into small pieces and ground using a pestle and mortar, with 250 ml of distilled water added gradually. The mixture was heated in a water bath at 60 °C for 4 hours until the solution turned reddish-brown. After cooling, the extract was filtered using Whatmann No.1 filter paper. The resulting filtrate was stored at 4 °C in a refrigerator for use in subsequent experiments.

Green Synthesis of NiO Nanoparticles: For the green synthesis of nickel oxide (NiO) nanoparticles, a precursor solution was prepared by dissolving 8 g of nickel nitrate in 100 ml of distilled water. This solution was then added drop wise to 100 ml of the rose leaf extract while stirring, continuously using a magnetic stirrer until a noticeable colour change occurred. After allowing the solution to cool to room temperature, it was incubated overnight. The mixture was then centrifuged at 3500 rpm three times, washing each time with distilled water to remove impurities. The resulting precipitate was collected and dried in a hot air oven at 300 °C until all moisture was eliminated. The dried NiO nanoparticles were stored in an airtight container for further analysis.

Characterization Studies

X-ray diffraction (XRD) was used to identify the crystalline phases of the synthesized NiO nanoparticles. The surface morphology and elemental composition were analyzed using Field Emission Scanning Electron Microscopy (FESEM) coupled with Energy Dispersive X-ray Spectroscopy (EDX). Optical properties were studied using a UV–VIS–NIR spectrophotometer within the wavelength range of 200–800 nm. Fourier-transform infrared (FTIR) spectroscopy was employed to identify the functional groups present in the samples.

XRD analysis: The crystal structure of the synthesized nanoparticles was determined and confirmed using X-ray diffraction (XRD) analysis. The XRD pattern of the as-synthesized nickel (II) oxide (NiO) nanoparticles is displayed in fig. 2, with the five most intense peaks summarized in table 2. The positions of the diffraction peaks correspond to a monoclinic phase, indicating the formation of a single-phase NiO structure without any detectable impurities. The broad nature of the peaks suggests the presence of nanoscale crystallites.

The crystallite sizes were estimated using the following formula:

$$D = \frac{0.9\,\lambda}{\beta cos\theta} \quad (1)$$

where D is the crystallite size, λ is the wave length of radiation, θ is the Bragg's angle and β is the full width at half maximum (FWHM). The estimated particle size is approximately 30 nm. The appearance of distinct, sharp peaks in the XRD pattern, along with the particle size being below 100 nm, confirms the nanocrystalline nature of the material.

FT-IR Analysis: Figure 3a and 3b display the FTIR spectra of the NiO nanoparticles, highlighting several prominent absorption peaks. The FTIR analysis of the synthesized nickel oxide nanoparticles was conducted over the wavelength range of 3800 cm^{-1} to 500 cm^{-1}. The spectra reveal two strong transmission bands at 529 cm^{-1} and 659 cm^{-1} which correspond to the characteristic structure of the NiO catalyst.

The peak at 529 cm^{-1} is attributed to the metal–oxygen (M–O) stretching vibration associated with octahedrally coordinated cobalt ions. Meanwhile, the band at 629 cm^{-1} arises from the M–O stretching vibration of tetrahedrally coordinated cadmium ions. A peak at 1401 cm^{-1} corresponds to the stretching vibration of nitrate ions (NO_3^-), indicating residual $Ni(NO_3)_2$. Additionally, the peak observed at 791 cm^{-1} is assigned to NiO.[8,19,20]

FESEM and EDX Analysis: Field Emission Scanning Electron Microscopy (FESEM) images of the nickel oxide nanoparticles prepared via the co-precipitation method are shown in fig. 4(a–d) at varying magnifications. The images reveal the formation of a flower-like morphology when the sample is calcined at 500 °C. Elemental composition was analyzed alongside FESEM using Energy Dispersive X-ray (EDX) spectroscopy. The EDX results confirmed the presence of elements consistent with nickel oxide nanoparticles, showing no evidence of impurities. This purity corroborates the phase identification obtained from the XRD analysis.[15]

Table 2
Peak wise XRD analysis

Peak No.	Xc 2θ	FWHM	D	Intensity
1	37.2418	0.57867	2.4591	27737.2
2	43.2936	0.60449	-2.4358	45585.87
3	62.9065	0.75099	1.8468	17295.33
4	75.4479	0.81758	1.6957	5285.91
5	90.4017	127.2873	0.0315	-6917.79

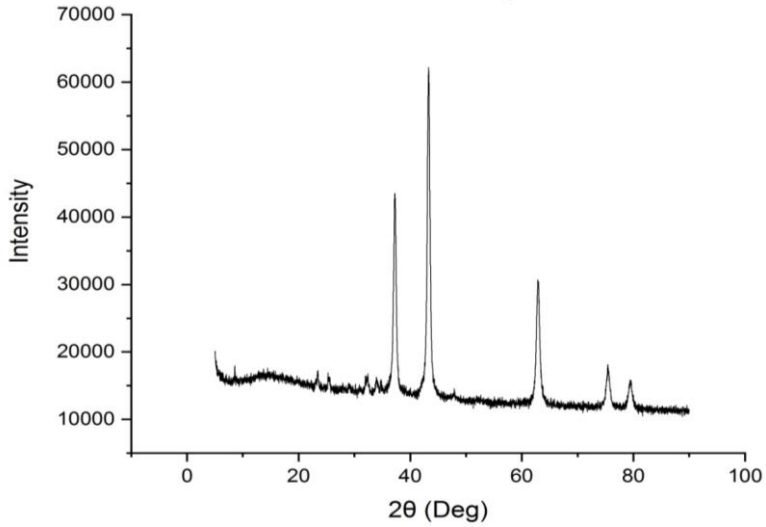

Fig. 2: XRD Spectra of NiO np's

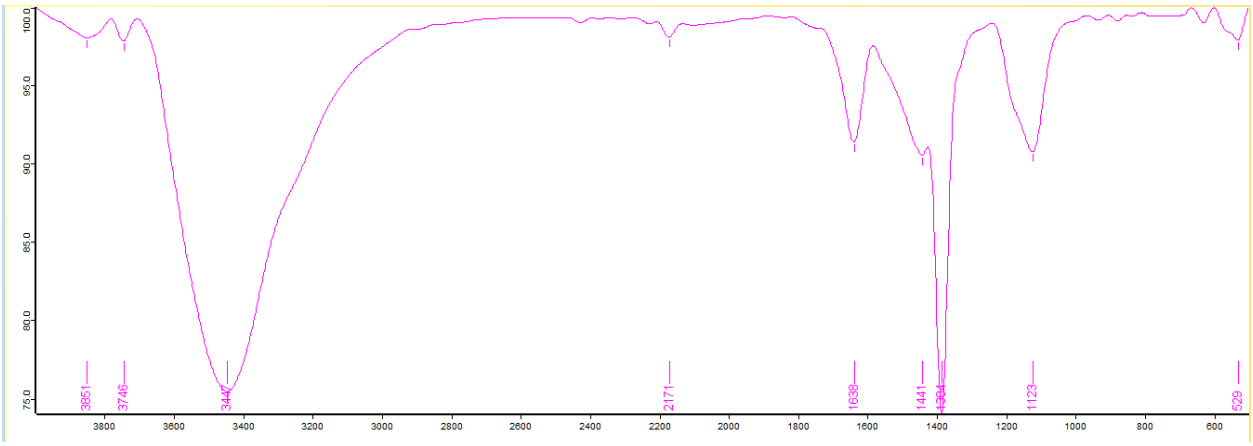

Fig. 3a: FTIR Spectra of NiO np's

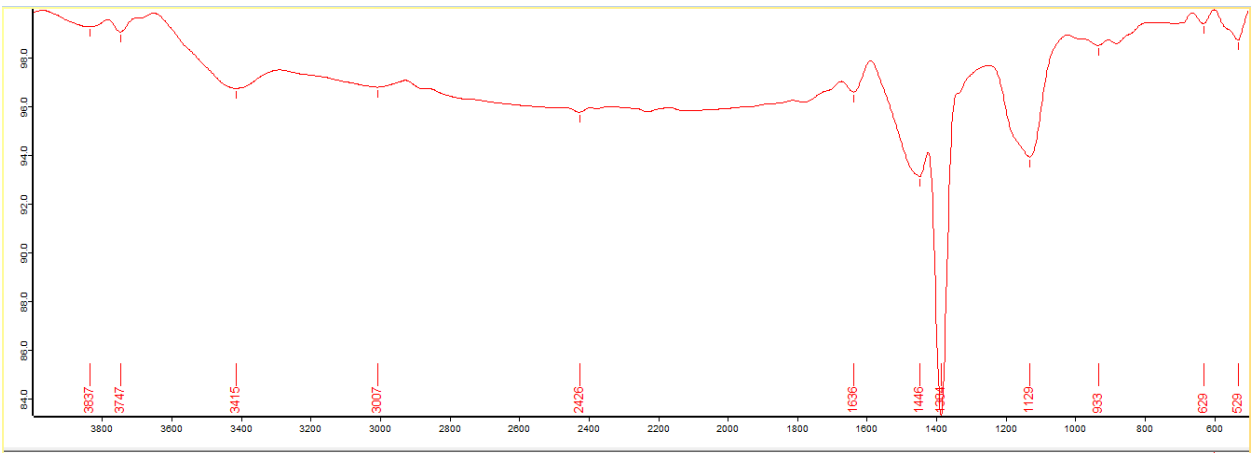

Fig. 3b: FTIR Spectra of NiO np's

Photocatalytic Performance Test

A stock solution of Fast Green dye (1×10^{-3} M) was prepared by dissolving 150 mg of Fast Green in 250 mL of double distilled water. The absorbance of this solution was measured using a spectrophotometer at its maximum wavelength of 625 nm. A diluted Fast Green dye solution with a concentration of 1.0×10^{-5} M was then prepared from the stock solution. Fifty millilitres of this diluted dye solution were divided equally into four separate beakers for different experimental conditions. The first beaker, containing only the dye solution, was kept in the dark. The second beaker, also containing the dye solution, was exposed to light without any catalyst.

The third beaker contained the dye solution along with 0.1 g of NiO nanoparticles (NiO NPs) and was kept in the dark. The fourth beaker contained both 0.1 g of NiO NPs and the dye solution and was irradiated with light. After 5 hours, the absorbance of the solutions from all four beakers was measured using a UV spectrophotometer. A noticeable decrease in absorbance was observed only in the fourth beaker, indicating that both NiO nanoparticles and light are necessary for the degradation of Fast Green dye. The other three beakers showed minimal or no change in absorbance.

Photocatalytic Degradation: A 3.0×10^{-5} M Fast Green dye solution was prepared using doubly distilled water, to which 0.150 g of nickel oxide nanoparticles were added. The pH of the mixture was adjusted to 4.0 using a standardized sodium hydroxide solution. The reaction mixture was irradiated using a 60-watt lamp. Samples of 2 mL were withdrawn at regular intervals and their optical density (OD) was recorded at 625 nm. It was observed that the OD of the dye solution decreased progressively with increasing exposure time, with almost complete degradation achieved after 6 hours of illumination. A plot of log OD versus time (seconds) showed a linear trend. The rate constant (k) was calculated using the formula: k = 2.303 × slope. Data from a representative experiment are provided in table 2.

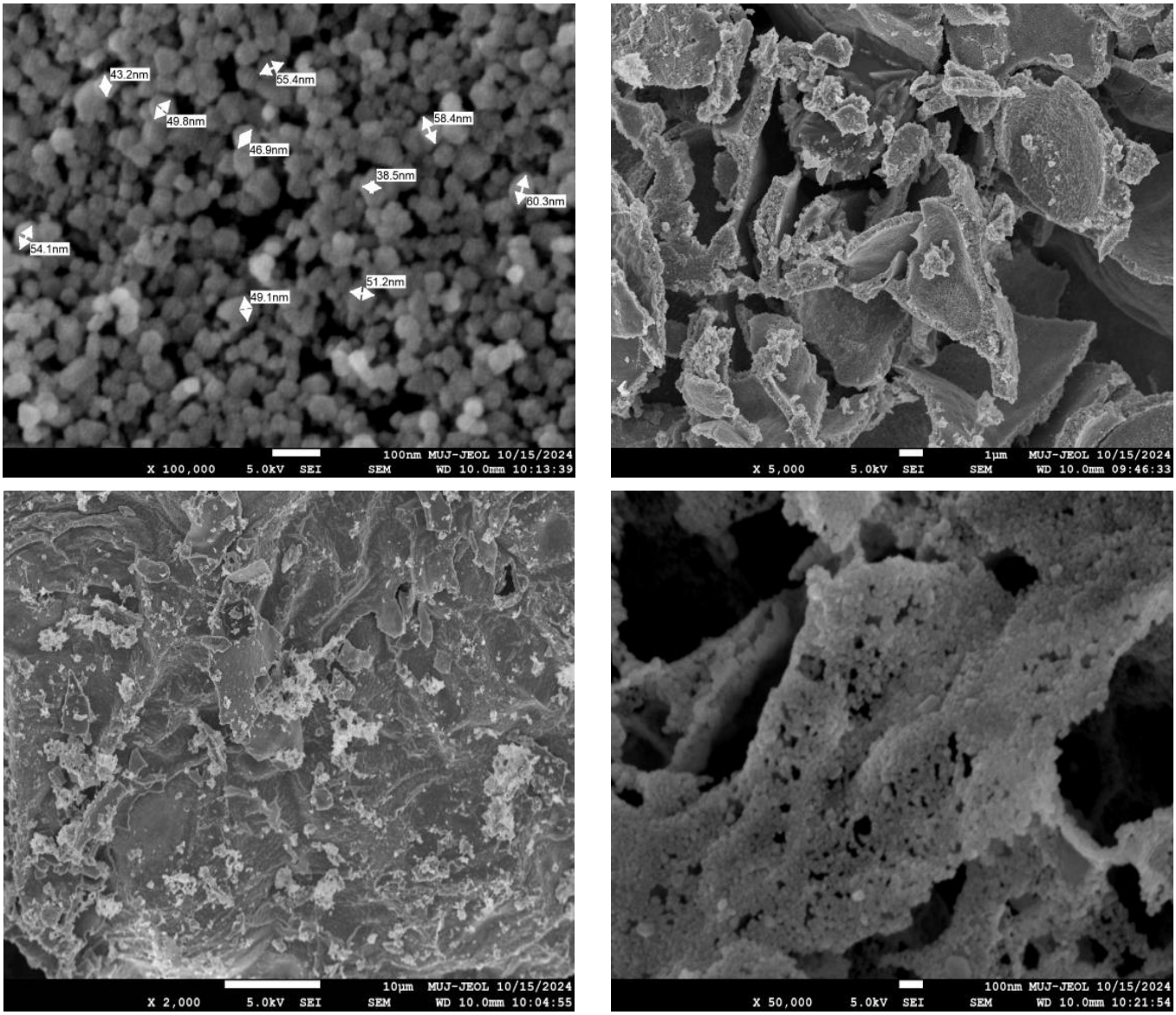

Fig. 4a,4b,4c and 4d: FESEM using EDX Image of NiO np's

Results and Discussion

Typical Run:

Fast Green Dye: 3.0×10^{-5} M	pH: 4.0
Light Intensity: 60 mW cm^{-2}	NiO NP's Dose: 0.150 g

Effect of pH: Photocatalytic degradation of any dye solution may be affected by the pH of the medium. pH was varied from 3.0 to 7.0. pH was measured using a digital pH meter. The pH of solution was varied by adding 1N HNO_3 and 1N NaOH solution. The effect of pH on the dye degradation with nickel oxide NP's is summarized in the table 3.

Fast Green Dye: 3.0×10^{-5} M	
Light Intensity: 60 mW cm^{-2}	NiO NP's Dose: 0.150 g

Table 3
Typical run

Time	Optical Density (OD)	1+log OD
0	0.914	0.960946
15	0.837	0.922725
30	0.734	0.865696
45	0.682	0.833784
60	0.609	0.784617
75	0.526	0.720986
90	0.483	0.683947
105	0.385	0.585461
120	0.311	0.49276
135	0.215	0.332438
150	0.186	0.269513

Rate Constant (k) = 1.733x 10^5Sec

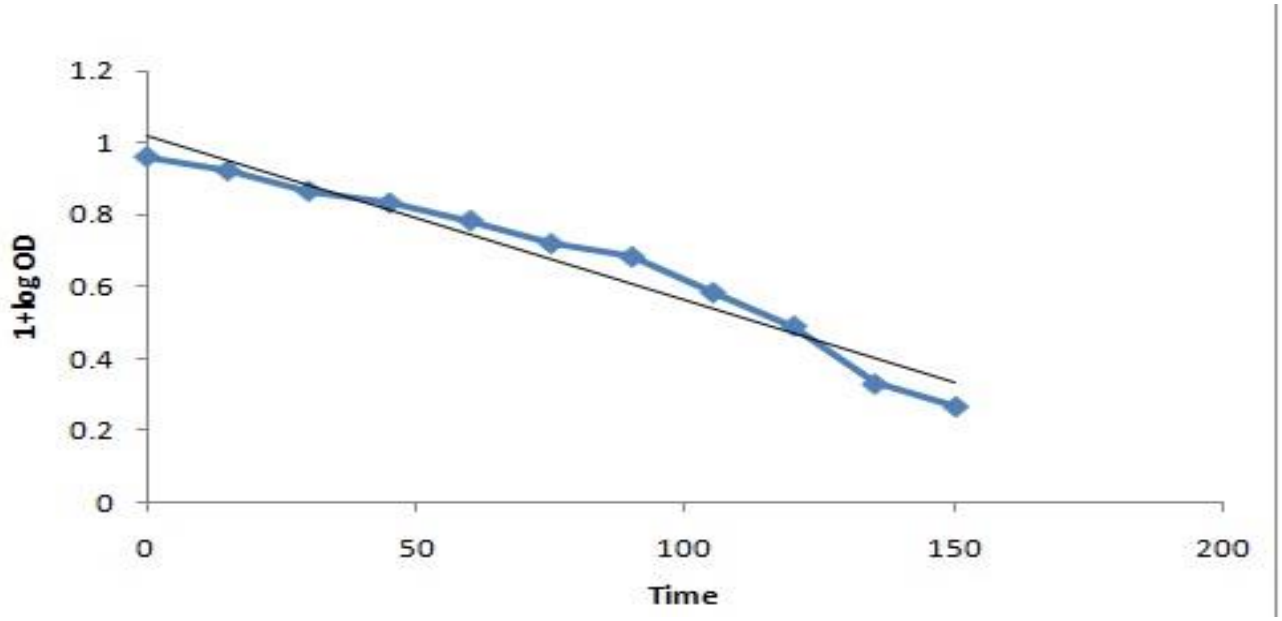

Fig. 5: Typical Run

Table 4
pH Variation

pH	k x 10^4
2	7.675171
3	10.29723
4	12.05882
5	11.60982
6	10.30594
7	8.563538

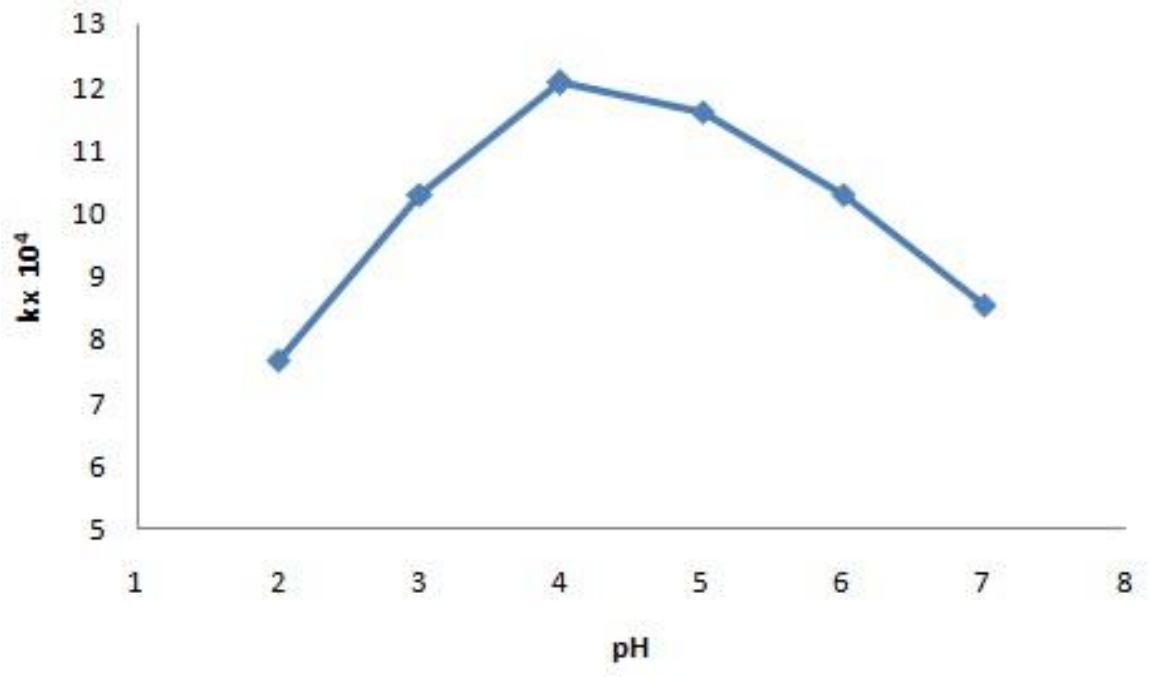

Fig. 6: pH variation

Effect of Dye Concentration: The dye concentration was varied between 0.5×10^{-5} M and 3.0×10^{-5} M. The rate of dye degradation increased steadily as the concentration rose up to 3.0×10^{-5} M, after which it gradually declined (Table 3). The photocatalytic activity improves with increasing dye concentration because more dye molecules are available for excitation and energy transfer, resulting in enhanced photoactivity. However, beyond this concentration, the dye begins to act as a filter, blocking the incoming light from reaching the catalyst surface, which leads to a reduction in photocatalytic efficiency.

	pH : 4.0
Light Intensity: 60 mW cm^{-2}	NiO NP's Dose: 0.150 g

Table 5
Variation with Dye Concentration

Dye Concentration (10^5)	k x 10^4
0.5	7.675171
1	10.51081
1.5	**12.12816**
2	11.65093
2.5	11.31322
3	9.421784

Effect of Light Intensity: The intensity of light also influences the rate of photo degradation. The light intensity varied from 20.0 to 100.0 mW/cm^{-2} and the results are tabulated in the table 6.

Fast Green Dye: 3.0×10^{-5} M	pH : 4.0
	NiO NP's Dose : 0.150 g

Table 6
Variation in Light Intensity

Light Intensity (mW cm^{-2})	k x 10^4
20	9.824823
40	10.76473
60	**11.86519**
80	10.50242
100	8.394412

Effect of Amount of Catalyst: The quantity of the photocatalyst, nickel oxide nanoparticles, also influences the photocatalytic degradation of Fast Green dye. The catalyst amount was varied from 0.025 g to 0.225 g. It was found that the degradation rate increased with the catalyst amount up to an optimum point, after which it further increases leading to a decline in the degradation rate. These findings are summarized in table 7.

Fast Green Dye : 3.0×10^{-5} M	pH : 4.0
Light Intensity : 60 mW cm^{-2}	

Table 7
Variation in NiO Dose

NiO Dose (mg)	k x 10^4
25	7.224589
50	8.013677
75	9.117957
100	10.60224
125	11.15129
150	**11.72552**
175	10.85998
200	9.661242
225	7.194225

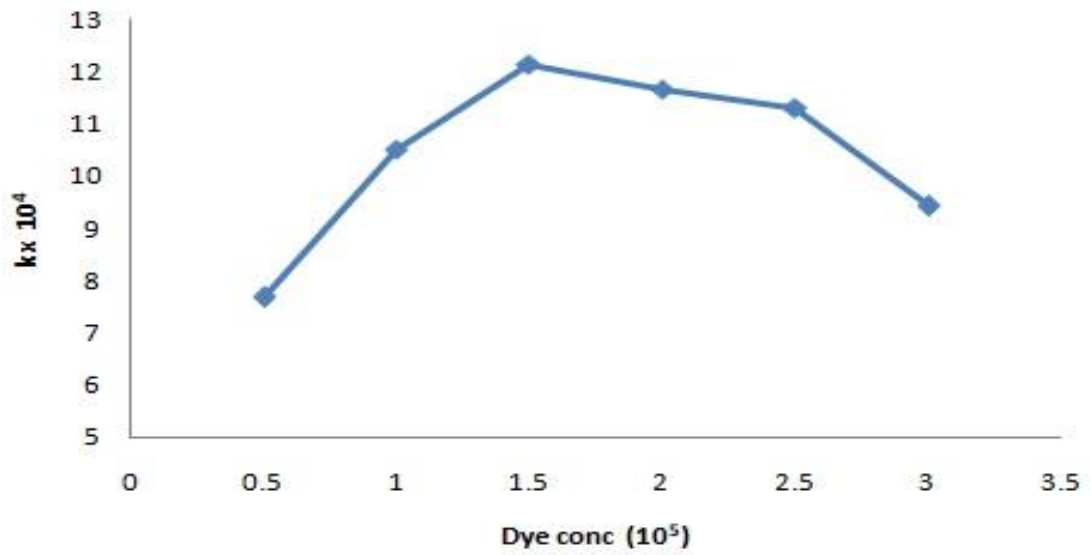

Fig. 7: Variation in Dye Concentration

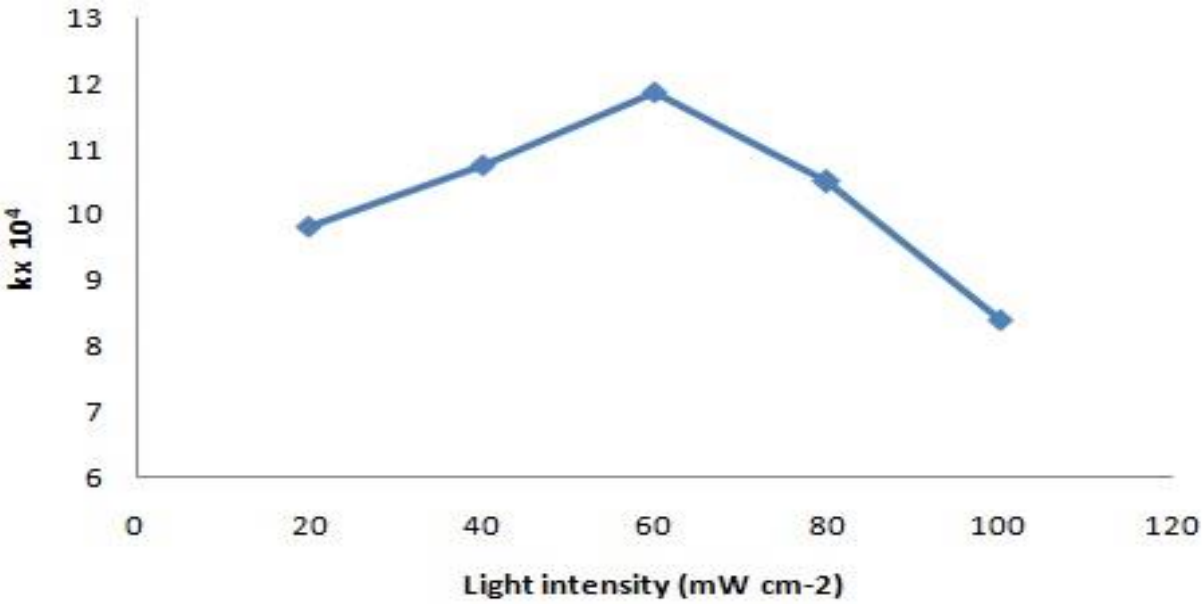

Fig. 8: Variation in Light Intensity

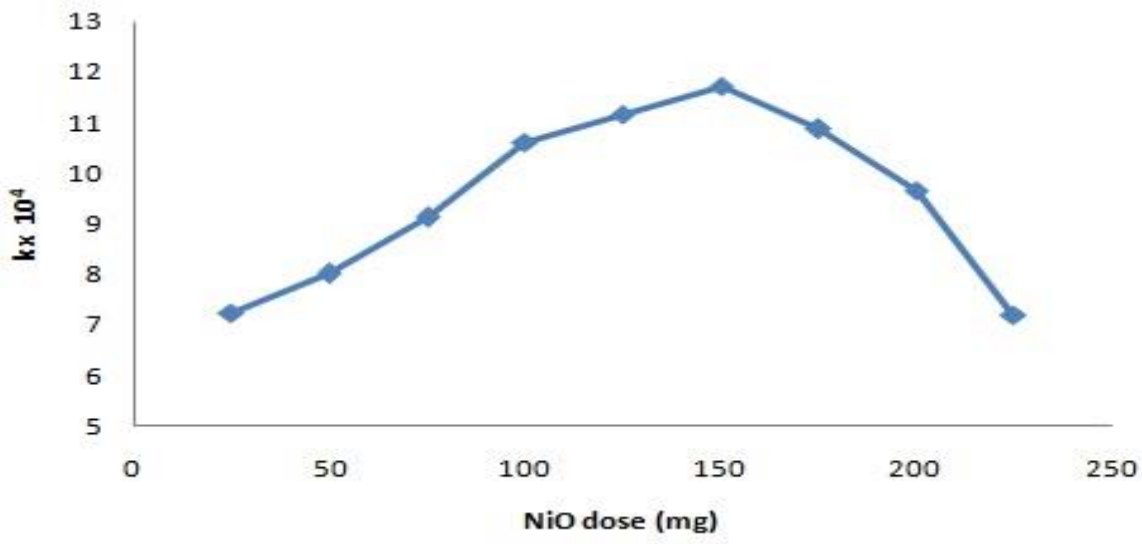

Fig. 9: Variation in NiO Dose

Conclusion

In conclusion, nickel oxide nanoparticles were successfully synthesized using both precipitation and green synthesis methods with nickel nitrate hexahydrate as the precursor. The resulting spinel-structured nickel nitrate exhibited a large specific surface area and demonstrated excellent photocatalytic performance in degrading fast green dye. The optimal conditions for the reaction were determined to be:

- pH = 4.0
- Fast Green concentration = 3.0×10^{-5} M
- NiO nanoparticles amount = 0.150 g
- Light intensity = 60.0 mW/cm^{-2}

Moreover, the nickel oxide nanoparticles maintained their photocatalytic efficiency for up to three reuse cycles, highlighting their potential for practical applications in environmental remediation.

References

1. Anand et al, Food Consumption and its Impact on Cardiovascular Disease: Importance of Solutions Focused on the Globalized Food System, *J Am Coll Cardiol.*, **66(14)**, 1590-1614, doi: 10.1016/j.jacc.2015.07.050 **(2015)**

2. Chen L., Lesmond D.A. and Wei J., Corporate Yield Spreads and Bond Liquidity, *The Journal of Finance*, https://doi.org/10.1111/j.1540-6261.2007.01203.x **(2007)**

3. Demirbas A., Agricultural Based Activated Carbons for the Removal of Dyes from Aqueous Solutions: A Review, *Journal of Hazardous Materials*, **167(1)**, 1–9, https://doi.org/10.1016 /j.jhazmat.2008.12.114 **(2009)**

4. Dippong T., Levei E.A. and Cadar O., Investigation of Structural, Morphological and Magnetic Properties of MFe2O4 (M = Co, Ni, Zn, Cu, Mn) Obtained by Thermal Decomposition, *Int J Mol Sci*, **23(15)**, 8483, https://doi.org/10.3390/ijms23158483 **(2022)**

5. Fazelirad H., Ranjbar M., Taher M.A. and Sargazi G., Preparation of magnetic multi-walled carbon nanotubes for an efficient adsorption and spectrophotometric determination of amoxicillin, *Journal of Industrial and Engineering Chemistry*, **21**, 889-892, https://doi.org/10.1016/j.jiec.2014.04.028 **(2015)**

6. Gligorovski S., Strekowski R., Barbati S. and Vione D., Environmental Implications of Hydroxyl Radicals ((•)OH), *Chem Rev*, **115(24)**, 13051–13092, https://doi.org/10.1021/cr500310b **(2015)**

7. Gu C.G. et al, Onset of cooperation between layered networks, *Physical Review E*, https://doi.org/10.1103/PhysRevE.84.026101 **(2011)**

8. Hoffmann M.R., Martin S.T., Choi W. and Bahnemann D.W., Environmental Applications of Semiconductor Photocatalysis, *Chem. Rev.*, **95(1)**, 69–96 **(1997)**

9. Hyeon T., Chemical Synthesis of Magnetic Nanoparticles, *Chem. Commun.*, 927–934, https://doi.org/10.1039/B207789B **(2003)**

10. Kannadasan N., Poonguzhali R. and Shanmugam N., Influence of thermal annealing on the photo catalytic properties of TiO2 nanoparticles under solar irradiation, *Journal of Materials Science: Materials in Electronics*, **26(10)**, 7987-7996 **(2015)**

11. Klissurski D.G. and Uzunova E.L., Synthesis of high-dispersity zinc cobaltite from coprecipitated hydroxycarbonate precursor, *Journal of Materials Science Letters*, **9(5)**, 576-579, https://colab.ws/articles/10.1007%2Fbf00725882 **(1990)**

12. Klissurski D. and Uzunova E., Synthesis of Nickel Cobaltite Spinel from Coprecipitated Nickel-Cobalt Hydroxide Carbonate, *Chem. Mater*., **3(6)**, 1060–1063, https://doi.org/10.1021/ cm00018a021 **(1991)**

13. Klissurski D. and Uzunova E., Synthesis and Features of Binary Cobaltite Spinels, *J Mater Sci*, **29(2)**, 285–293, https://doi.org/10.1007/BF01162484 **(1994)**

14. Martin D.J., Liu G., Moniz S.J.A., Bi Y., Beale A.M., Ye J. and Tang J., Efficient Visible Driven Photocatalyst, Silver Phosphate: Performance, Understanding and Perspective, *Chem. Soc. Rev*., **44(21)**, 7808–7828, https://doi.org/10.1039 /C5CS00380F **(2015)**

15. Nakata K., Ochiai T., Murakami T. and Fujishima A., Photoenergy Conversion with TiO2 Photocatalysis: New Materials and Recent Applications, *Electrochimica Acta*, **84**, 103–111, https://doi.org/10.1016/j.electacta.2012.03.035 **(2012)**

16. Nemiwal M., Zhang T.C. and Kumar D., Recent progress in g-C3N4, TiO2 and ZnO based photocatalysts for dye degradation: Strategies to improve photocatalytic activity, *Sci Total Environ*., **767**, 144896, doi: 10.1016/j.scitotenv.2020.144896 **(2021)**

17. Ni M., Leung M.K.H., Leung D.Y.C. and Sumathy K., A review and recent developments in photocatalytic water-splitting using TiO2 for hydrogen production, *Renewable Sustainable Energy Reviews*, **11(3)**, 401–425, https://doi.org/10.1016/ j.rser.2005.01.009 **(2007)**

18. Paike V.V., Niphadkar P.S., Bokade V.V. and Joshi P.N., Synthesis of Spinel CoFe2O4 Via the Co-Precipitation Method Using Tetraalkyl Ammonium Hydroxides as Precipitating Agents, *Journal of the American Ceramic Society*, **90(9)**, 3009–3012, https://doi.org/10.1111/j.1551-2916.2007.01843.x **(2007)**

19. Paliwal G. and Sharma M., Photocatalytic degradation of nigrosin dye using rose flower extract mediated nickel oxide nanoparticles, *International Journal of Food and Nutritional Sciences*, **13(4)**, 1602–1611 **(2022)**

20. Schneider J., Matsuoka M., Takeuchi M., Zhang J., Horiuchi Y., Anpo M. and Bahnemann D.W., Understanding TiO2 Photocatalysis: Mechanisms and Materials, *Chem Rev*, **114(19)**, 9919–9986, https://doi.org/10.1021/cr5001892 **(2014)**

21. Srivastava Sweta, Pathak A.D., Mall A.K. and Singh Rachana, Enumeration, Identification and characterization of endophytic bacteria isolated from sugar beet (Beta vulgaris L.) root for ethanol production, *Res. J. Biotech*., **19(6)**, 13-18, https://doi.org/10.25303/1906rjbt013018 **(2024)**

22. Tachikawa T. and Majima T., Single-Molecule, Single-Particle Fluorescence Imaging of TiO2-Based Photocatalytic Reactions,

Chem. Soc. Rev., **39(12)**, 4802–4819, https://doi.org/10.1039/B919698F **(2010)**

23. Turkin A.I. and Drebushchak V.A., Synthesis and Calorimetric Investigation of Stoichiometric Fe-Spinels: MgFe2O4, *Journal of Crystal Growth*, **265(1)**, 165–167, https://doi.org/10.1016/j.jcrysgro.2004.01.037 **(2004)**.

(Received 17th July 2025, accepted 21st August 2025)